Available online at www.sciencedirect.com
SCIENCE DIRECT®
PERGAMON
International Journal of Heat and Mass Transfer 46 (2003) 4003–4011
International Journal of HEAT and MASS TRANSFER
www.elsevier.com/locate/ijhmt

Effect of uniform suction on laminar filmwise condensation on a finite-size horizontal flat surface in a porous medium

Shih-Chieh Wang, Yue-Tzu Yang, Cha'o-Kuang Chen *

Department of Mechanical Engineering, National Cheng Kung University, Tainan 701, Taiwan, ROC

Received 1 November 2002; received in revised form 28 April 2003

Abstract

The theoretical analysis of filmwise condensation outside a finite-size horizontal flat surface embedded in a porous medium filled with a dry saturated vapor has been solved by a boundary layer treatment. The Newton–Raphson scheme was employed to solve the finite-size horizontal flat plate in porous medium. Results turns out that the average Nusselt number for condensation heat transfer is expressed in terms of Darcy number, Jakob number, film liquid Prandtl number, Darcy-modified Rayleigh number and the parameter of suction, as well as are given for the condensate layer thickness profiles.

Keywords: Laminar filmwise condensation; Porous medium; Stokes flow

1. Introduction

The vapor transfer with condensation in porous medium is of practical importance in various fields of application. For examples, these are the design of evaporative condensers, enhanced recovery of petroleum resources, civil engineering, functional clothing design, geothermal reservoirs, and other industrial applications.

Since the pioneering investigator Nusselt [1] in 1916, the problem of vapor filmwise condensation on vertical wall has been subjected to four major assumptions. The Nusselt problem has been improved the above assumptions over the years by Rohsenow [2], Sparrow and Gregg [3], Churchill [4], Chen [5], and Koh et al. [6,7], etc. Denny and Mills [8] based on the Nusselt assumptions have been stretched to include the effects of (i) forced vapor flow, (ii) variable wall temperatures, and (iii) variable fluid properties.

Jain and Bankoff [9] used a double power perturbation method to get an exact solution of the Nusselt problem with constant suction velocity. Their results showed that the increase in heat transfer from suction can be effected laminar film condensation on a porous vertical wall. Char et al. [10] used the Darcy–Brinkman–Forchheimer (DBF model) to treat the condensate field in a porous medium and found the local heat transfer rate increased with a decrease in the Jakob number, the Peclet number, and the inertial parameter or an increased in the conjugate heat transfer parameter. Popov [11] inquired into laminar film condensation on a horizontal flat surface in 1951. His experimental results showed considerable scatter, possibly owing to non-condensable gases. Gerstmann and Griffith [12] studied condensation on the underside of horizontal and inclined surface both theoretically and experimentally. Leppert and Nimmo [13], and Shigechi et al. [14] investigated laminar condensation on the upper side of a horizontal flat plate. Yang and Chen [15] used the concept of hydraulics of open channel flow to search the boundary condition of the plate edge. Recently, Yang and coworkers [16,17] considered condensation on a

* Corresponding author. Tel.: +886-3-275-7575x62140; fax: +886-6-234-2081.
E-mail address: ckchen@mail.ncku.edu.tw (C.-K. Chen).

0017-9310/03/$ - see front matter © 2003 Published by Elsevier Ltd.
doi:10.1016/S0017-9310(03)00247-3

Nomenclature

C	constant
C_p	specific heat at constant pressure
Da	the Darcy number defined in Eq. (20)
g	acceleration of gravity
h	heat transfer coefficient
h_{fg}	latent heat of condensation
Ja	the Jakob number defined in Eq. (20)
k	effective thermal conductivity
K	intrinsic permeability of a porous medium
L	finite-size horizontal flat surface length
$\dot{m}$	condensate mass flow rate defined in Eq. (15)
Nu	Nusselt number defined in Eq. (33)
P	pressure
Pr	the Prandtl number defined in Eq. (20)
q	heat flux defined in Eq. (31)
Ra	the Darcy-modified Rayleigh number defined in Eq. (20)
Re_w	the Reynolds number at surface defined in Eq. (20)
S_w	the suction parameter at surface defined in Eq. (20)
T	temperature
ΔT	saturation temperature minus surface temperature
u	the Darcian velocity in x-direction
v	the Darcian velocity in y-direction
v_w	suction velocity on the plate surface
x	axial coordinate
Y	function defined in Eq. (30) or (41)
y	transverse coordinate

Greek symbols

α	thermal diffusivity of a porous medium
δ	local condensate layer thickness
ε	porosity of a porous medium
η	dimensionless condensate layer thickness defined by δ/δ_0
λ	parameter is defied as $\lambda = h_{fg} + 0.5C_p\Delta T$
μ	effective viscosity of condensate layer
ρ	density of condensate layer

Superscripts

$*$	indicates dimensionless quantity
–	indicates average quantity

Subscripts

0	quantity at the flat surface center
c	quantity at the flat surface edge
ef	effective properties due to a porous medium
L	quantity at the flat surface edge
n	iteration
r	relative quantity
s	saturated properties
w	finite-size horizontal flat surface
x	local properties

finite-size horizontal wavy disk and plate facing upward with previous concept [15]. The concept, which is from Bakhmeteff's [18] writings, is the minimum mechanical energy with respect to the boundary layer thickness at the edge of the plate.

In the present study, the laminar film condensation on a finite-size, horizontal, permeable, flat plate in a porous medium filled with dry saturated vapor was investigated. Owing to the larger porosities adjacent to solid surface result in reduction of the resistance to the flow; the non-uniformities near the boundary will pay an importance role in the condensate flow at the plate surface. Hence, we consider uniformities of a porous medium that lead to the Darcy model for the condensate flow in a porous medium. The dimensionless average Nusselt number and the condensate layer thickness on the plate surface are examined at different values of the governing parameters those are the Darcy number Da (i.e. permeability), the Jakob number Ja (i.e. thermal resistance across condensate layer), the Prandtl number Pr (i.e. physical properties of film liquid), the Rayleigh number Ra (i.e. laminar flow) and the suction parameter S_w.

2. Analysis

A schematic diagram of the physical model and coordinate system is shown in Fig. 1. A porous horizontal clean flat surface is maintained at constant temperature T_w. The gas is a pure quiescent vapor at a uniform temperature T_s. When the temperature of permeable plate surface is lower than the saturation temperature T_s

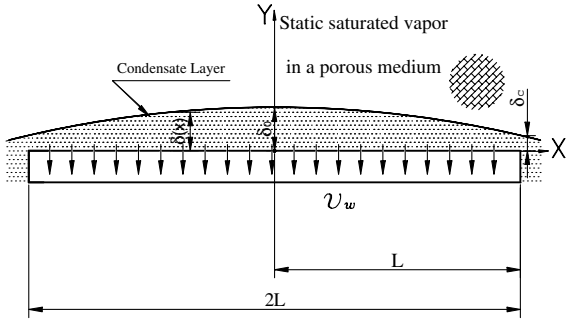

Fig. 1. Physical model and coordinate system.

of a pure vapor and when nucleation sites are offered, condensation commences, and if the liquid wets the surface ideally, thereupon, film condensation occurs on the flat plate. In order to achieve our ultimate goal of finding heat transfer results, it is necessary to analyze the velocity and temperature distributions in the condensate layer. The flow of condensate depends on the variation in hydrostatic pressure. The momentum boundary layer is furthermore subject to a uniform suction which removes the condensate at a constant suction velocity. For this work, the local volume-averaged conservation equations are approved. The analysis of film condensation about a horizontal flat surface in a porous medium is developed under the following assumptions:

(1) Darcy's law is applicable to both the dry vapor and liquid phases in the porous medium.
(2) The condensate is incompressible fluid and the variations of the properties of porous medium, the dry vapor and condensate film are neglected.
(3) The viscous dissipation term in energy equation is neglected, as well as the radiation, chemical reaction, and electromagnetic effects.
(4) The convective liquid, vapor and the porous medium are in local thermodynamic equilibrium at every location in the system.
(5) The local film thickness is larger than the pore or particle size of a porous medium.
(6) The shear stress and surface tension at the liquid–vapor, liquid–solid, and vapor–solid interfaces are assumed to be negligible.
(7) The effect of non-condensable gas is insignificant.
(8) The change in momentum flow within the vapor boundary layer is neglected.

The governing equations with boundary layer simplifications are given as:

continuity equation:

$$\frac{\partial u}{\partial x}+\frac{\partial v}{\partial y}=0 \tag{1}$$

momentum x-direction:

$$u=\left(\frac{K}{\mu_{\mathrm{ef}}}\right)\left(-\frac{\partial P}{\partial x}\right) \tag{2}$$

y-direction:

$$0=-\frac{\partial P}{\partial y}-\rho g \tag{3}$$

energy equation:

$$u\frac{\partial T}{\partial x}+v\frac{\partial T}{\partial y}=\alpha_{\mathrm{ef}}\frac{\partial^2 T}{\partial y^2} \tag{4}$$

where u and v are the Darcian velocity components in the x- and y-directions, respectively, K denotes the intrinsic permeability of porous medium and the dimension of K is in square of length (e.g., m^2), P is the pressure of liquid, g is the gravitational acceleration, ρ is the density of condensate layer, μ_{ef} and α_{ef} are the effective dynamic viscosity and effective thermal diffusivity of a porous medium saturated with liquid, respectively. The Eq. (2) states a linear relationship that is characteristic of the Stokes flow. Noting that the velocity in the pores is higher than the Darcy velocity by $1/\varepsilon$, where ε is the porosity (e.g., the volume fraction occupied by voids). These Eqs. (1)–(4) are subjected to the following boundary conditions:

At the flat surface ($y=0$):

$$T=T_w \tag{5}$$

where T_w is always a specified temperature.

At the vapor–liquid interface ($y=\delta(x)$):

$$T=T_{\mathrm{s}},\quad P=P_{\mathrm{s}} \tag{6}$$

where T_{s} is the saturated temperature of a vapor, P_{s} is the saturated pressure under the temperature T_{s}, $\delta(x)$ is the local condensate layer thickness which is to be determined.

Now, the static pressure gradient term can be obtained by integrating Eq. (3) with the use of boundary condition Eq. (6) gives,

$$P=P_{\mathrm{s}}+\rho g[\delta(x)-y] \tag{7}$$

In the meanwhile, substituting Eq. (7) into Eq. (2), one can solve the x- directional velocity profile can be solved as follows:

$$u=\left(\frac{\rho g K}{\mu_{\mathrm{ef}}}\right)\left(-\frac{\mathrm{d}\delta}{\mathrm{d}x}\right) \tag{8}$$

In accordance with the first law of thermodynamics, Fourier's conduction law and Nusselt theory, these lead to the governing equations for the energy balance in the film:

$$k\left.\frac{\partial T}{\partial y}\right|_{y=0}=\rho v_w(h_{\mathrm{fg}}+C_{\mathrm{p}}\Delta T)+\frac{\mathrm{d}}{\mathrm{d}x}\left[\int_0^{\delta(x)}\rho u[h_{\mathrm{fg}}+C_{\mathrm{p}}(T_{\mathrm{s}}-T)]\,\mathrm{d}y\right] \tag{9}$$

where k is the effective thermal conductivity of the fluid saturated porous medium, h_{fg} is the latent heat of condensation, and C_{p} is the specific heat of condensate at constant pressure. It is assumed that v_w is a constant related to both the magnitude direction of the normal velocity at the plate; $v_w>0$, suction and $v_w<0$, injection, where the direction according to Fig. 1. If the condensate layer thickness $\delta(x)$ is relatively small compared with the length of the plate L, the temperature profile can be considered to be the following form:

$$T=\frac{y}{\delta}\Delta T+T_w \tag{10}$$

where ΔT is the saturation temperature minus surface temperature (e.g., $\Delta T = T_s - T_w$). In Eq. (10) obviously satisfies the energy Eq. (4) and boundary condition Eqs. (5) and (6).

Substituting Eqs. (8) and (10) into Eq. (9), the governing equation can be expressed as

$$\delta\frac{\mathrm{d}}{\mathrm{d}x}\left(\delta\frac{\mathrm{d}\delta}{\mathrm{d}x}\right) = -\left(\frac{k\mu_{\mathrm{ef}}}{\rho^2 gK}\right)\frac{\Delta T}{(h_{\mathrm{fg}} + 0.5C_{\mathrm{p}}\Delta T)} + \left(\frac{v_w\mu_{\mathrm{ef}}}{\rho gK}\right)\frac{(h_{\mathrm{fg}} + C_{\mathrm{p}}\Delta T)}{(h_{\mathrm{fg}} + 0.5C_{\mathrm{p}}\Delta T)}\delta \tag{11}$$

Its corresponding boundary conditions yield

$$\frac{\mathrm{d}\delta}{\mathrm{d}x} = 0 \quad \text{at } x = 0 \tag{12}$$

and

$$\delta = \delta_{\mathrm{c}} \quad \text{at } x = L \tag{13}$$

where δ_{c} is the condensate layer thickness at the edge of flat surface, which is still unknown. One cannot solve Eq. (11) with its boundary conditions yet. The edge thickness δ_{c} need not become zero when the system is in steady state steady flow process. In accordance with a minimum mechanical energy principle, presented by Bakhmeteff [18], one would find a new boundary condition to solve Eq. (11). That one has the following equation:

$$\frac{\partial}{\partial\delta_{\mathrm{c}}}\left(\int_0^{\delta(x)}\left(\frac{u^2}{2} + gy + \frac{P}{\rho}\right)\rho u\,\mathrm{d}y\right)\bigg|_{\dot{m}=\dot{m}_{\mathrm{c}}} = 0 \tag{14}$$

where $\dot{m}_{\mathrm{c}}$ is the critical value of mass flow out of the plate edge. The rate of condensate mass flow at any section x should become as

$$\dot{m} = \int_0^{\delta(x)}\rho u\,\mathrm{d}y \tag{15}$$

And the substitution of Eq. (8) gives as follows:

$$\dot{m} = \left(\frac{\rho^2 gK}{\mu_{\mathrm{ef}}}\right)\delta(x)\left(-\frac{\mathrm{d}\delta}{\mathrm{d}x}\right) \tag{16}$$

$$\dot{m}_{\mathrm{c}} = \left(\frac{\rho^2 gK}{\mu_{\mathrm{ef}}}\right)\delta_{\mathrm{c}}\left(-\frac{\mathrm{d}\delta}{\mathrm{d}x}\right)\bigg|_{x=L} \tag{17}$$

By solving Eq. (14) subject to boundary conditions Eqs. (13) and (17), we can obtain the following relation term:

$$\dot{m}_{\mathrm{c}}^2 = \rho^2 g\delta_{\mathrm{c}}^3 \tag{18}$$

Combining Eqs. (17) and (18) yields the new boundary condition:

$$\left(-\frac{\mathrm{d}\delta}{\mathrm{d}x}\right)\bigg|_{x=L} = \left(\frac{\mu_{\mathrm{ef}}^2\delta_{\mathrm{c}}}{\rho^2 gK^2}\right)^{1/2} \tag{19}$$

With an aim of assisting the analysis, these following transformations are innovated to non-dimensionalize the preceding equations

$$\begin{aligned} &x^* = \frac{x}{L}, \quad \eta = \frac{\delta}{\delta_0}, \quad \eta_{\mathrm{r}} = \frac{\delta_{\mathrm{c}}}{\delta_0}, \quad \delta_L^* = \frac{L}{\delta_0},\\ &Pr = \frac{\mu_{\mathrm{ef}}C_{\mathrm{p}}}{k}, \quad S_w = \frac{PrRe_w}{Ja}(1 + 0.5Ja),\\ &Ra = \frac{\rho^2 gPrL^3}{\mu_{\mathrm{ef}}^2}, \quad Ja = \frac{C_{\mathrm{p}}\Delta T}{\lambda}, \quad Da = \frac{K}{L^2},\\ &Re_w = \pm\frac{\rho v_w L}{\mu_{\mathrm{ef}}}, \quad u^* = \frac{u}{\sqrt{gL}} \end{aligned} \tag{20}$$

where $\lambda = h_{\mathrm{fg}} + 0.5C_{\mathrm{p}}\Delta T$, η_{r} is the relative thickness of condensate, Pr is the Prandtl number, Ra is the Darcy-modified Rayleigh number, Ja is the Jakob number, Da is the Darcy number, Re_w is the Reynolds number which $Re_w > 0$ for suction or blowing at the flat surface. The Jakob number is a measure of the relative degree of subcooling in the condensate. In terms of the new variables, the Eq. (19) of boundary condition becomes non-dimensionalize boundary condition

$$\left.\frac{\mathrm{d}\eta}{\mathrm{d}x^*}\right|_{x^*=1} = -\sqrt{\frac{Pr\eta_{\mathrm{r}}}{Da^2Ra\delta_L^*}} \tag{21}$$

The governing Eq. (11) and its boundary conditions Eqs. (12) and (13) can transform to:

$$\eta\frac{\mathrm{d}}{\mathrm{d}x^*}\left(\eta\frac{\mathrm{d}\eta}{\mathrm{d}x^*}\right) = \left(\frac{Ja\delta_L^{*3}}{DaRa}\right)(S_w\eta - 1) \tag{22}$$

$$\frac{\mathrm{d}\eta}{\mathrm{d}x^*} = 0, \quad \text{at } x^* = 0 \tag{23}$$

$$\eta = \eta_{\mathrm{r}}, \quad \text{at } x^* = 1 \tag{24}$$

According with Eqs. (8) and (20), the dimensionless velocity in the x-direction is defined as

$$u^*(x^*) = \sqrt{\frac{JaDa\delta_L^*}{Pr}}\frac{\sqrt{2[1 - \eta(x^*)] - S_w[1 - \eta(x^*)^2]}}{\eta(x^*)} \tag{25}$$

Case 1. Let the value of velocity v_w of lateral mass flux on plate surface be zero.

If one neglected the suction effect, then we could set that $S_w = 0$. Employing a new transformation in Eq. (22), carrying out integrations and rearranging, we obtain:

$$(2 + \eta)^2(1 - \eta) = \left(\frac{9Ja\delta_L^{*3}}{2DaRa}\right)x^{*2} \tag{26}$$

$$\left.\frac{\mathrm{d}\eta}{\mathrm{d}x^*}\right|_{x^*=1} = -\sqrt{\frac{2Ja\delta_L^{*3}(1 - \eta_{\mathrm{c}})}{DaRa\eta_{\mathrm{r}}^2}} \tag{27}$$

where $0 < \eta_{\mathrm{c}} \leqslant 1$.

In virtue of boundary condition Eq. (21) has to be equal to Eq. (27), with some rearrangement one achieves

$$Pr\eta_{\mathrm{r}}^3 - 2JaDa\delta_L^{*4}(1 - \eta_{\mathrm{r}}) = 0 \tag{28}$$

Substituting Eq. (24) into Eq. (26), then having used Eq. (28) to eliminate δ_L^*, we obtain the following governing equation:

$$(1-\eta_r)^7(2+\eta_r)^8 = \frac{6561}{128}\left(\frac{JaPr^3}{Da^7Ra^4}\right)\eta_r^9 \tag{29}$$

At the same time, we set the following equation to check the existence of η_r:

$$Y(\eta_r) = (1-\eta_r)^7(2+\eta_r)^8 - \frac{6561}{128}\left(\frac{JaPr^3}{Da^7Ra^4}\right)\eta_r^9 \tag{30}$$

According to Fourier's law of heat conduction, the local heat flux $q_w(x)$ to the plate can be computed by the following equation:

$$q_w(x) = k\left.\frac{\partial T}{\partial y}\right|_{y=0} = k\frac{\Delta T}{\delta(x)} \tag{31}$$

Hence, in terms of the transformed variables of this work, the surface dimensionless local heat flux $q_w^*(x^*)$ can be expressed as

$$q_w^*(x^*) = \frac{q_w(x)L}{k\Delta T} = \frac{\delta_L^*}{\eta(x^*)} \tag{32}$$

The local Nusselt number Nu_x is defined as

$$Nu_x = \frac{Lh_x}{k} = \frac{q_w(x)L}{k\Delta T} = \frac{\delta_L^*}{\eta(x^*)} \tag{33}$$

where h_x is the local heat transfer coefficient.

The average heat transfer coefficient $\bar{h}$ over the length L of the plate would be written as

$$\bar{h} = \frac{1}{L}\int_0^L h_x\,dx = \frac{k}{L}\int_0^L \frac{1}{\delta(x)}\,dx = \frac{k}{\delta_0}\int_0^1 \frac{1}{\eta(x^*)}\,dx^* \tag{34}$$

The average Nusselt number $\overline{Nu}$ can be obtained by integrating the local Nusselt number Nu_x Eq. (33) over the plate surface. This can be defined as

$$\overline{Nu} = \frac{L\bar{h}}{k} = \int_0^1 \frac{\delta_L^*}{\eta(x^*)}\,dx^* \tag{35}$$

In this case, the $\overline{Nu}$ can be rewritten as

$$\overline{Nu} = -\sqrt{\frac{DaRa}{2Ja\delta_L^*}}\int_1^{\eta_r}\frac{d\eta}{\sqrt{1-\eta}} = \sqrt{\frac{2DaRa(1-\eta_r)}{Ja\delta_L^*}} \tag{36}$$

Case 2. Let the value of suction velocity v_w be a constant.

In this case, with Eq. (22) and its appropriate boundary conditions, we have the following solution equation (37) and the new boundary condition Eq. (38):

$$\sqrt{\frac{JaS_w^3\delta_L^{*3}}{DaRa}}x^* = Ln\left(\frac{1-S_w}{1-S_w\eta-\sqrt{S_w(1-\eta)[2-S_w(1+\eta)]}}\right) - \sqrt{S_w(1-\eta)[2-S_w(1+\eta)]} \tag{37}$$

$$\left.\frac{d\eta}{dx^*}\right|_{x^*=1} = -\sqrt{\frac{Ja\delta_L^{*3}[2(1-\eta_r)-S_w(1-\eta_r^2)]}{DaRa\eta_r^2}} \tag{38}$$

Because the boundary condition Eq. (21) has to be equal to Eq. (38), we would better take some rearrangements:

$$Pr\eta_r^3 - JaDa\delta_L^{*4}[2(1-\eta_r)-S_w(1-\eta_r^2)] = 0 \tag{39}$$

When Eqs. (37) and (39) and boundary condition Eq. (24) are used to eliminate δ_L^*, we obtain the following equation:

$$\sqrt{S_w(1-\eta_r)[2-S_w(1+\eta_r)]} + \sqrt{\frac{JaS_w^3}{DaRa}}\left(\frac{Pr\eta_r^3}{JaDa(1-\eta_r)[2-S_w(1+\eta_r)]}\right)^{3/8} + Ln\left(\frac{1-S_w\eta_r-\sqrt{S_w(1-\eta_r)[2-S_w(1+\eta_r)]}}{1-S_w}\right) = 0 \tag{40}$$

Otherwise, we set the following equation

$$Y(\eta_r) = \sqrt{S_w(1-\eta_r)[2-S_w(1+\eta_r)]} + \sqrt{\frac{JaS_w^3}{DaRa}}\left(\frac{Pr\eta_r^3}{JaDa(1-\eta_r)[2-S_w(1+\eta_r)]}\right)^{3/8} + Ln\left(\frac{1-S_w\eta_r-\sqrt{S_w(1-\eta_r)[2-S_w(1+\eta_r)]}}{1-S_w}\right) \tag{41}$$

In terms of Eq. (35), the average Nusselt number $\overline{Nu}$ in the Case 2 will be expressed as

$$\overline{Nu} = -\sqrt{\frac{DaRa\delta_0}{JaL}}\int_1^{\eta_c}\frac{d\eta}{\sqrt{2(1-\eta)-S_w(1-\eta^2)}} = -\sqrt{\frac{DaRa}{JaS_w\delta_L^*}} \times Ln\left[\frac{1-S_w\eta_c-\sqrt{S_w[2(1-\eta_c)-S_w(1-\eta_c^2)]}}{1-S_w}\right] \tag{42}$$

3. Results and discussion

In Case 1, from the Eq. (29), we set the Eq. (30) which to plot the Fig. 2 and to check the existence of

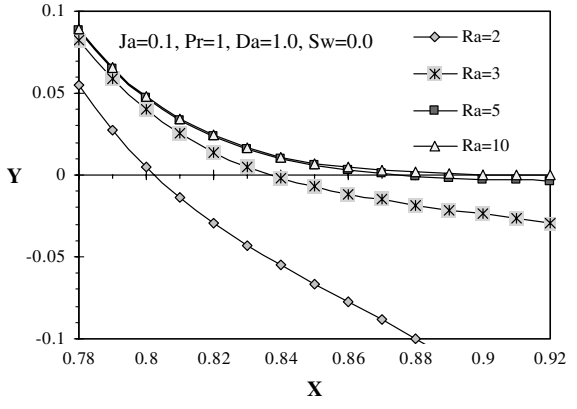

Fig. 2. In Case 1, variation of $\eta_c = X$ at different values of Rayleigh numbers Ra for $Ja = 0.1$, $Pr = 1$, $Da = 1$, and $S_w = 0$.

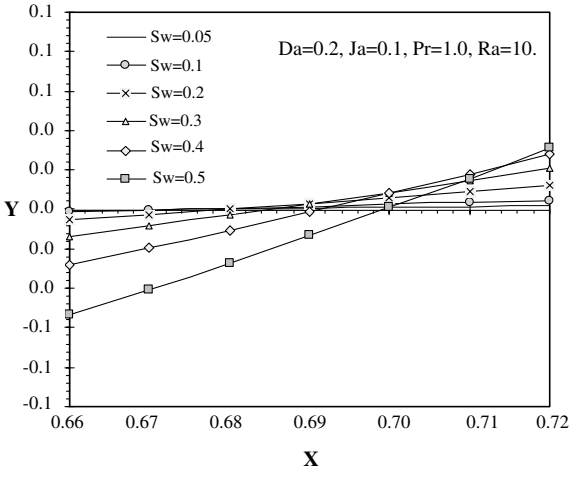

Fig. 3. In Case 2, variation of $\eta_c = X$ at different values of suction parameters S_w for $Ja = 0.1$, $Pr = 1$, $Da = 0.2$, and $Ra = 10$.

solutions. Fig. 2 shows that the solution values of relative thickness η_r $(= X)$ increase with Rayleigh number Ra and are reflected the physical problem that have a unique solution for specifying parameters. In a meanwhile, in Case 2, it is essential to know that there is at most one solution in Eq. (40) or not for specifying parameters. Therefore, we would use the Eq. (41) to plot Fig. 3. With respect to Fig. 3 it is seen that the solution η_r $(= X)$ of Eq. (41) exists only one for logical conditions and has $0.68 \leqslant \eta_r \leqslant 0.72$ for various S_w, when given $Ja = 0.1$, $Pr = 1.0$, $Ra = 10$, and $Da = 0.2$. In addition, we can find that, these values of solution increase with suction parameter S_w.

Numerical solution in this problem is obtained by using the Newton–Raphson scheme. For Cases 1 and 2, the value of initial estimate $\eta_r = 0.9999$ and the relative absolute change $|(\eta_r)_{n+1} - (\eta_r)_n|/|(\eta_r)_n| \leqslant 10^{-8}$ are used to any specified parameters. It is pertinent to note that $S_w = 0$ corresponds to considering an impermeable plate without suction. Here the Prandtl number varies from very little vales for liquid metals to very large values for ordinary liquids and oils is considered. When the Darcy number $Da = 0.2$, the Jakob number $Ja = 0.01$, and the suction parameter $S_w = 0.1$ are selected, the values of η_r and $1/\delta_L^*$ for various values of Prandtl number Pr, and Darcy-modified Rayleigh number Ra are shown in Tables 1 and 2, respectively. It can be seen that the value of η_r decreases as Pr increases and η_r increases with Ra on account of the lower effective viscosity. Besides, the central condensate thickness of horizontal plate decreases as Pr increases, and also $1/\delta_L^*$ decreases as Ra increases. The smaller value of $1/\delta_L^*$ manifests the central condensate film thickness δ_0 of the plate length L is very thin, where L is a large-scale characteristic length. The higher value of η_r discloses the condensate layer thickness variations are very small for higher Ra. As far as Fig. 4 is concerned, it is clear that the variation of δ/δ_0 $(= \eta)$ with x^* is more significant with decreasing Ra, i.e. the high variation of curvature of condensate profile is due to increasing the effective viscosity. The higher effective viscosity leads to the liquid velocities which are extremely small. It also should be made known that the variation of condensate profile η shows insignificant those effects of suction for $Ra \geqslant 100$.

The heat transfer results thus obtained are exhibited on Figs. 5–9. Fig. 5 shows the effects of the suction Sw on the local Nusselt number Nu_x for $Da = 0.2$, $Ja = 0.01$, and $Pr = 0.1$. From the Fig. 5, it can be seen that Nu_x increases with x^*, Ra and Sw. It also should be pointed out that the variation of Nu_x between $Sw = 0.5$ and $Sw = 0$ for $Ra = 100$ shows more significant than for $Ra = 1$. In other word, the effect of suction for higher Darcy-modified Rayleigh number is superior to for lower Ra.

Fig. 6 shows the average Nusselt number $\overline{Nu}$ expressed in terms of Rayleigh number Ra for $Da = 0.2$ and $Pr = 0.1$, when the effect of suction does exist or not. This indicates that at a fixed Ra with a given Sw, the value of $\overline{Nu}$ for low Ja by contrast with the value of $\overline{Nu}$ for high Ja is effective, i.e. the suction effectiveness is more significant for little thermal resistance across condensate layer $(C_p \Delta T/h_{fg} \ll 1)$. On the other hand from Fig. 6, it is seen that the variation of $\overline{Nu}$ for low Rayleigh number liquids does exist much larger than for high Rayleigh number liquids, i.e. when in the range of $0 < Ra \leqslant 1000$ the liquid velocities are all little on the ground of the high effective local drag force.

In Fig. 7, the solid lines represent the theoretical predictions of the average Nusselt $\overline{Nu}$ when the effect of suction is not considered. This illustrates the role of the thermal resistance across condensate layer (i.e. Ja) on

Table 1
Values of η_c when $Ja = 0.01$, $Da = 0.2$, $S_w = 0.1$ for Case 2

$\eta_c = \delta_c/\delta_0$	$Ja = 0.01$, $Da = 0.2$, $S_w = 0.1$				
	$Pr = 10$	$Pr = 5$	$Pr = 1$	$Pr = 0.5$	$Pr = 0.1$
$Ra = 1$	0.241348	0.293428	0.441077	0.512293	0.674653
$Ra = 10$	0.520031	0.591759	0.742401	0.795264	0.886056
$Ra = 100$	0.800435	0.843955	0.915434	0.935856	0.966829
$Ra = 500$	0.91006	0.931687	0.964602	0.973475	0.986528
$Ra = 1000$	0.937751	0.953047	0.97592	0.982006	0.990897
$Ra = 2000$	0.957297	0.967945	0.983677	0.987825	0.993857
$Ra = 5000$	0.974288	0.980778	0.99027	0.992754	0.996353
$Ra = 10000$	0.982561	0.986989	0.993433	0.995113	0.997543

Table 2
Values of δ_0/L when $Ja = 0.01$, $Da = 0.2$, $S_w = 0.1$ for Case 2

δ_0/L	$Ja = 0.01$, $Da = 0.2$, $S_w = 0.1$				
	$Pr = 10$	$Pr = 5$	$Pr = 1$	$Pr = 0.5$	$Pr = 0.1$
$Ra = 1$	0.377212	0.380343	0.394319	0.404703	0.443912
$Ra = 10$	0.188458	0.195159	0.218965	0.233333	0.277548
$Ra = 100$	0.109094	0.117177	0.141307	0.154206	0.190744
$Ra = 500$	0.081059	0.088393	0.109213	0.119995	0.149945
$Ra = 1000$	0.072263	0.079104	0.098305	0.108178	0.135489
$Ra = 2000$	0.064738	0.071058	0.088662	0.097671	0.122521
$Ra = 5000$	0.056267	0.061904	0.077507	0.085461	0.107344
$Ra = 10000$	0.050733	0.05588	0.070081	0.077306	0.097162

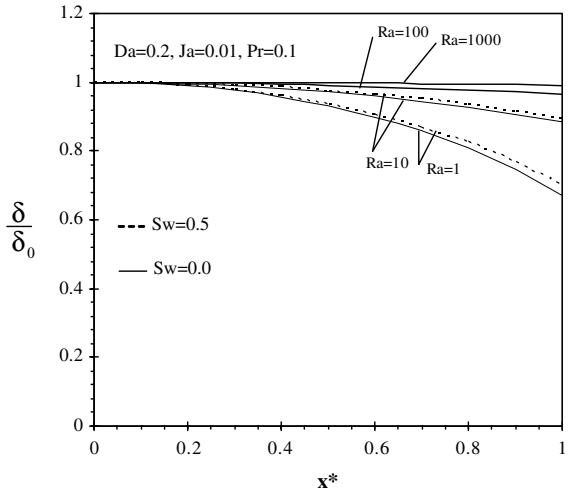

Fig. 4. Results for $Da = 0.2$, $Ja = 0.01$, and $Pr = 0.1$: dimensionless film profiles at different values of suction parameters S_w and Rayleigh number Ra.

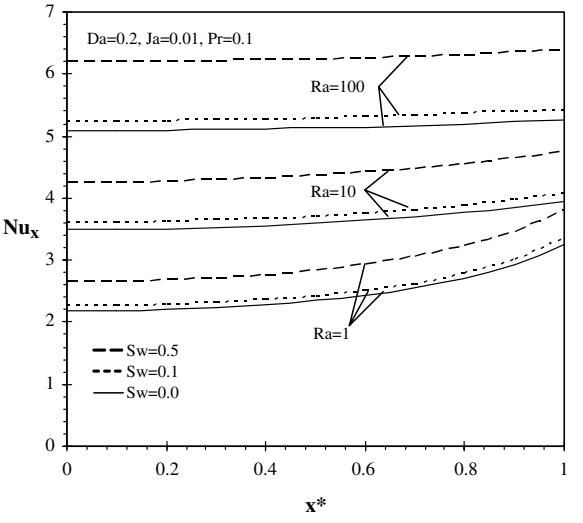

Fig. 5. Results for $Da = 0.2$, $Ja = 0.01$, and $Pr = 0.1$: the local Nusselt number Nu_x at different values of suction parameters S_w and Rayleigh number Ra.

the effects of dimensionless average heat flux $\overline{Nu}$. It can be seen that $\overline{Nu}$ variations and suction effects increase as the Jakob number decreases for $Ra = 1000$ and $Da = 0.2$. In addition, we can find that increasing values of the Ja there are decreasing deviations form linearity. Accordingly, it is concludes that both increasing suction effect and decreasing thermal resistance have better effects on the heat transfer rate.

In Fig. 8, it is seen that the values of $\overline{Nu}$ increases with Pr at different values of suction parameter S_w and Jakob number Ja for $Da = 1.0$ and $Ra = 5000$. It is can

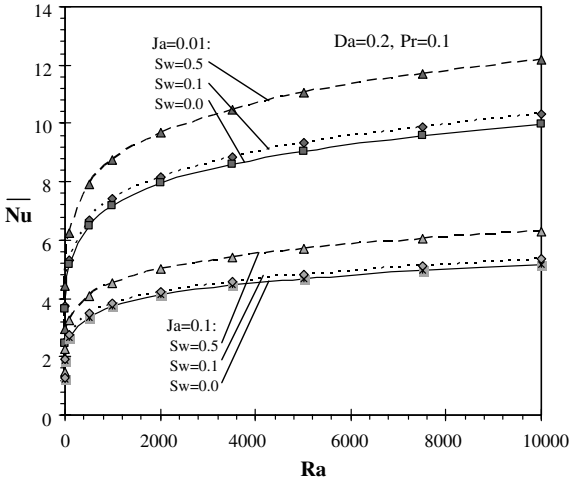

Fig. 6. Variation of Nusselt number $\overline{Nu}$ with Rayleigh number Ra at different values of Jakob number Ja and suction parameter S_w for $Pr = 0.1$, and $Da = 0.2$.

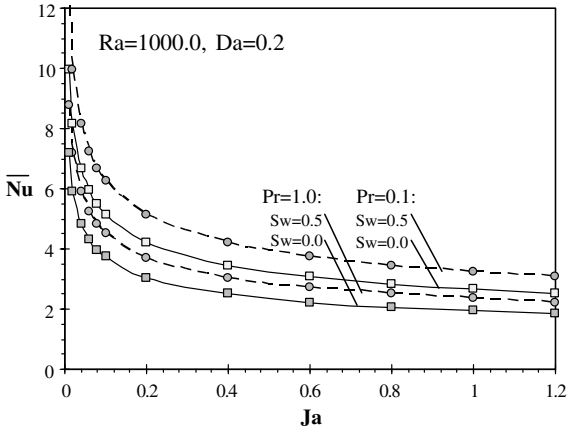

Fig. 7. Variation of Nusselt number $\overline{Nu}$ with Jakob number Ja at different values of Prandtl number Pr and suction parameter S_w for $Ra = 1000$, and $Da = 0.2$.

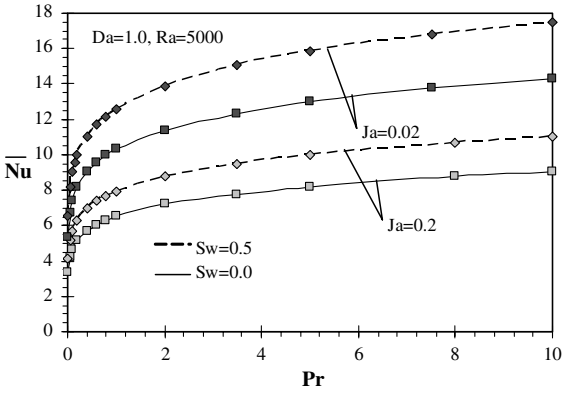

Fig. 8. Variation of Nusselt number $\overline{Nu}$ with Prandtl number Pr at different values of suction parameter S_w and Jakob number Ja for $Da = 1.0$ and $Ra = 5000$.

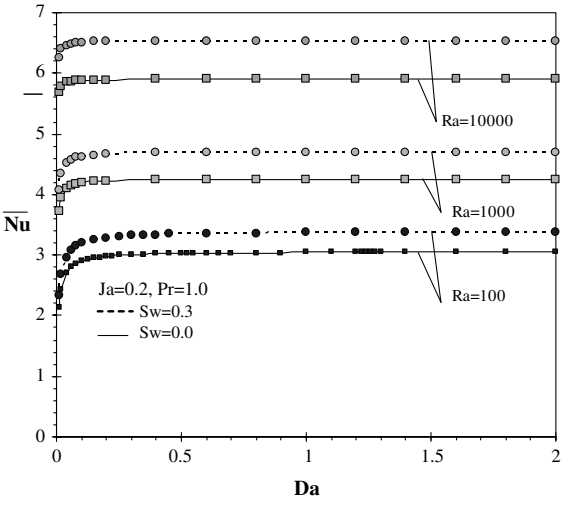

Fig. 9. Variation of Nusselt number $\overline{Nu}$ with Darcy number Da at different values of suction parameter S_w and Rayleigh number Ra for $Ja = 0.2$ and $Pr = 1$.

be observed form Fig. 9 that the values of $\overline{Nu}$ increases with Da, and $\overline{Nu}$ variations are almost no difference as $Da \geqslant 0.5$ at different values of suction parameter S_w and Rayleigh number Ra for $Ja = 0.2$ and $Pr = 1$. Base on these Figs. 6–8, we can find the scales for $\overline{Nu}$ are

$$\overline{Nu} \sim Ra^{1/7} \tag{43}$$

$$\overline{Nu} \sim Pr^{1/7} \tag{44}$$

$$\overline{Nu} \sim Ja^{-2/7} \tag{45}$$

As a result, all the $\overline{Nu}$ can be plotted as a functional relation in the form

$$\overline{Nu} = f(Ja^{-2/7}, Pr^{1/7}, Ra^{1/7}, Sw) \tag{46}$$

According to the curve fitting method and a functional relation Eq. (46), we can precisely predict the value of $\overline{Nu}$ for various suction parameters S_w, in the criterion $Ra \geqslant 1000$, $Da \geqslant 0.5$:

$$\overline{Nu} = C\frac{Pr^{1/7}Ra^{1/7}}{Ja^{2/7}} \tag{47}$$

where $C = 1.0$ for $S_w = 0.0$, $C = 1.03$ for $S_w = 0.1$, $C = 1.066$ for $S_w = 0.2$, $C = 1.107$ for $S_w = 0.3$, $C = 1.155$ for $S_w = 0.4$, and $C = 1.216$ for $S_w = 0.5$. It implies that these constants of C already include an effect of the intrinsic permeability of a porous medium. The value of the group parameter $\overline{Nu}/(Pr^{1/7}Ra^{1/7}Ja^{-2/7})$ with S_w for $Ra \geqslant 1000$, $Da \geqslant 0.5$ is shown in Fig. 10. It

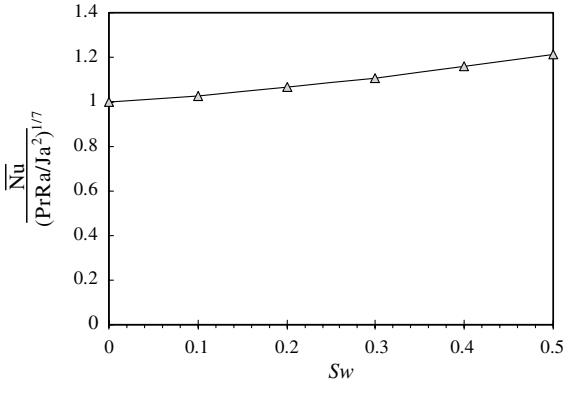

Fig. 10. The variation of suction effect $\overline{Nu}/(Pr^{1/7}Ra^{1/7}Ja^{-2/7})$ with S_w for $Ra \geqslant 1000$, $Da \geqslant 0.5$.

can be seen that the suction effect for heat transfer rate increases with suction parameter S_w.

4. Conclusions

This analysis performed, provides a fundamental understanding of a two-dimensional, finite-size, horizontal, permeable flat plate imbedded in a saturated porous medium. The criterion for the convergence of the solutions is that the relative absolute change $|(\eta_r)_{n+1} - (\eta_r)_n|/|(\eta_r)_n| \leqslant 10^{-8}$ is satisfied, otherwise, the solutions are very difficult to obtain for high Rayleigh number Ra with high Darcy number Da cases. The results indicate that the condensate thickness δ_0 at the plate center decreases as the suction parameter S_w increases. If we include the surface tension effects, the center thickness δ_0 at the plate center and the critical thickness δ_c at the plate edge will become larger. The Darcy number shows insignificant the effects of heat transfer for $Ra \geqslant 1000$ and $Da \geqslant 0.5$, thus, we can use the Nusselt correlation Eq. (47) to predict the average heat transfer coefficient in the form

$$\bar{h} = C\frac{k}{L}\left[\frac{\rho^2 g L^3 (2h_{fg}+1)^2}{4(\mu_{ef}C_p\Delta T)^2}\right]^{1/7}$$

for $Ra \geqslant 1000$ and $Da \geqslant 0.5$

where $C = 1.0$ for $S_w = 0.0$, $C = 1.03$ for $S_w = 0.1$, $C = 1.066$ for $S_w = 0.2$, $C = 1.107$ for $S_w = 0.3$, $C = 1.155$ for $S_w = 0.4$, and $C = 1.216$ for $S_w = 0.5$.

References

[1] W. Nusselt, Die Oberflächen-Kondensation des Wasserdampfes, Zeit. Ver. D. Ing. 60 (1916) 541–569.
[2] W.M. Rohsenow, Heat transfer and temperature distribution in laminar film condensation, Trans. ASME, J. Heat Transfer 78 (1956) 1645–1648.
[3] E.M. Sparrow, J.L. Gregg, A boundary-layer treatment of laminar film condensation, Trans. ASME, J. Heat Transfer 8 (1959) 13–18.
[4] S.W. Churchill, Laminar film condensation, Int. J. Heat Mass Transfer 29 (1986) 1219–1226.
[5] M.M. Chen, An analytical study of laminar film condensation: part 1—flat plates, Trans. ASME, J. Heat Transfer 83 (1961) 48–54.
[6] J.C.Y. Koh, An integral treatment of two-phase boundary layer in film condensation, Trans. ASME, J. Heat Transfer 83 (1961) 359–362.
[7] J.C.Y. Koh, E.M. Sparrow, J.P. Hartnett, The two phase boundary layer in laminar film condensation, Int. J. Heat Mass Transfer 2 (1961) 359–362.
[8] V.E. Denny, A.F. Mills, Nonsimilar solutions for laminar film condensation on a vertical surface, Int. J. Heat Mass Transfer 12 (1969) 965–979.
[9] K.C. Jain, S.G. Bankoff, Laminar film condensation on a porous vertical with uniform suction velocity, Trans. ASME, J. Heat Transfer 86 (1964) 481–489.
[10] M.I. Char, J.D. Lin, H.T. Chen, Conjugate mixed convection laminar non-Darcy film condensation along a vertical plate in a porous medium, Int. J. Eng. Sci. 39 (2001) 897–912.
[11] V.D. Popov, Heat transfer during vapor condensation on a horizontal surface, Trudy Kiew. Tecknol. Inst. Pishch. Prom. 11 (1951) 87–97.
[12] J. Gerstmann, P. Griffith, Laminar film condensation on the underside of horizontal and inclined surface, Int. J. Heat Mass Transfer 10 (1967) 567–580.
[13] G. Leppert, P. Griffith, Laminar film condensation on surface normal to body or inertial forces, Trans. ASME, J. Heat Transfer 80 (1968) 178–179.
[14] T. Shigechi et al., Film condensation heat transfer on a finite-size horizontal plate facing upward, Trans. JSME Ser. B 56 (1990) 205–210.
[15] S.-A. Yang, C.-K. Chen, Laminar film condensation on a finite-size horizontal plate with suction at the wall, Appl. Math. Model. 16 (1992) 325–329.
[16] Y.-T. Yang, C.-K. Chen, P.-T. Hsu, Laminar film condensation on a finite-size horizontal wavy disk, Appl. Math. Model. 21 (1997) 139–144.
[17] P.-T. Hsu, Y.-T. Yang, C.-K. Chen, Laminar film condensation on a finite-size horizontal wavy plate, Int. Comm. Heat Mass Transfer 24 (1997) 1141–1152.
[18] B.A. Bakhmeteff, Hydraulics of Open Channels, McGraw-Hill, New York, 1966, pp. 39–41.